Biosensors and Bioelectronics 165 (2020) 112285

Contents lists available at ScienceDirect

Biosensors and Bioelectronics

journal homepage: http://www.elsevier.com/locate/bios

# Selection of a metal ligand modified DNAzyme for detecting $Ni^{2+}$

Wei Ren [a,b], Po-Jung Jimmy Huang [b], Donatien de Rochambeau [c], Woohyun J. Moon [b], Jinyi Zhang [b], Mingsheng Lyu [a,d], Shujun Wang [a,d], Hanadi Sleiman [c], Juewen Liu [b,*]

[a] Jiangsu Key Laboratory of Marine Bioresources and Environment, Jiangsu Ocean University, Lianyungang, 222005, China
[b] Department of Chemistry, University of Waterloo, Waterloo, Ontario, N2L 3G1, Canada
[c] Department of Chemistry, McGill University, 801 Sherbrooke Street West, Montréal, Québec, H3A 0B8, Canada
[d] Co-Innovation Center of Jiangsu Marine Bio-industry Technology, Jiangsu Ocean University, Lianyungang, Jiangsu, 222005, China

ARTICLE INFO

*Keywords:*
Biosensors
DNAzymes
Aptamers
Fluorescence
SELEX

ABSTRACT

Nickel is a highly important metal, and the detection of $Ni^{2+}$ using biosensors is a long-stand analytical challenge. DNA has been widely used for metal detection, although no DNA-based sensors were reported for $Ni^{2+}$. DNAzymes are DNA-based catalysts, and they recruit metal ions for catalysis. In this work, in vitro selection of RNA-cleaving DNAzymes was carried out using a library containing a region of 50 random nucleotides in the presence of $Ni^{2+}$. To increase $Ni^{2+}$ binding, a glycyl–histidine-functionalized tertiary amine moiety was inserted at the cleavage junction. A representative DNAzyme named Ni03 showed a high cleavage yield with $Ni^{2+}$ and it was further studied. After truncation, the optimal sequence of Ni03l could bind one $Ni^{2+}$ or two $Co^{2+}$ for catalysis, while other metal ions were inactive. Its cleavage rates for 100 μM $Ni^{2+}$ reached 0.63 $h^{-1}$ at pH 8.0. A catalytic beacon biosensor was designed by labeling a fluorophore and a quencher on the Ni03l DNAzyme. Fluorescence enhancement was observed in the presence of $Ni^{2+}$ with a detection limit of 12.9 μM. The sensor was also tested in spiked Lake Ontario water achieving a similar sensitivity. This is another example of using single-site modified DNAzyme for sensing transition metal ions.

## 1. Introduction

Nickel is a highly important metal widely used in alloys, coating, catalysis, and plating (Dubal et al., 2015). The high consumption of nickel-containing products inevitably leads to environmental pollution. Exposure to nickel can result in a variety of adverse health effects such as skin allergies, lung fibrosis, damages to kidney and cardiovascular system, and cancer (Denkhaus and Salnikow, 2002). Therefore, detection of $Ni^{2+}$ is an important analytical task. $Ni^{2+}$ can be detected using analytical instruments such as inductively-coupled plasma atomic emission or mass spectrometry. A complementary method is to develop sensors and biosensors for portable, on-site and real-time detection.

Rational design of $Ni^{2+}$ chelators has been reported. For example, Alizadeh and coworkers synthesized 1-p-tolyl-3-(3-(trifluoromethyl) phenyl)triaz-1-ene 1-oxide, but it also reacted with $Pb^{2+}$, $Co^{2+}$ and $Zn^{2+}$ (Alizadeh et al., 2014). Li and coworkers reported a colorimetric assay of $Ni^{2+}$ using a glutathione-stabilized silver nanoparticles with a detection limit of 75 μM $Ni^{2+}$, but it was interfered by $Co^{2+}$ and $Cd^{2+}$ (Li et al., 2009). A circular dichroism based sensor was also reported using L-cysteine-functionalized quantum dots, but it responded to both $Ni^{2+}$ and $Co^{2+}$ (Tedsana et al., 2015). Aside from the specificity problem, most of these sensors required a fraction of organic solvents or immobilization to achieve high sensitivity.

DNA has been shown to be an excellent ligand for metal sensing (Zhang et al., 2011; Zhou et al., 2017). DNA is highly stable, cost-effective to synthesize, and easy to modify compared to antibodies (Kahn et al., 2017; McConnell et al., 2020a; Qing et al., 2019; Zhang et al., 2020). In particular, for metal ion detection, DNA has unique advantages. While DNA has been shown to detect a large number of metal ions with excellent sensitivity and selectivity, detection of $Ni^{2+}$ remains a major challenge in the field. We cannot find DNA aptamers in the literature for binding $Ni^{2+}$, although a few in vitro selected and natural RNA aptamers exist were reported (Furukawa et al., 2015; Hofmann et al., 1997). However, DNA is preferred since RNA is unstable and too expensive for practical applications outside cells. Relying solely on binding, aptamers may suffer from non-specific metal binding since DNA is highly negatively charged (He et al., 2018; Hwang et al., 2016; Sigel and Sigel, 2010).

* Corresponding author.
*E-mail address:* liujw@uwaterloo.ca (J. Liu).

https://doi.org/10.1016/j.bios.2020.112285
Received 2 March 2020; Received in revised form 28 April 2020; Accepted 7 May 2020
Available online 18 May 2020

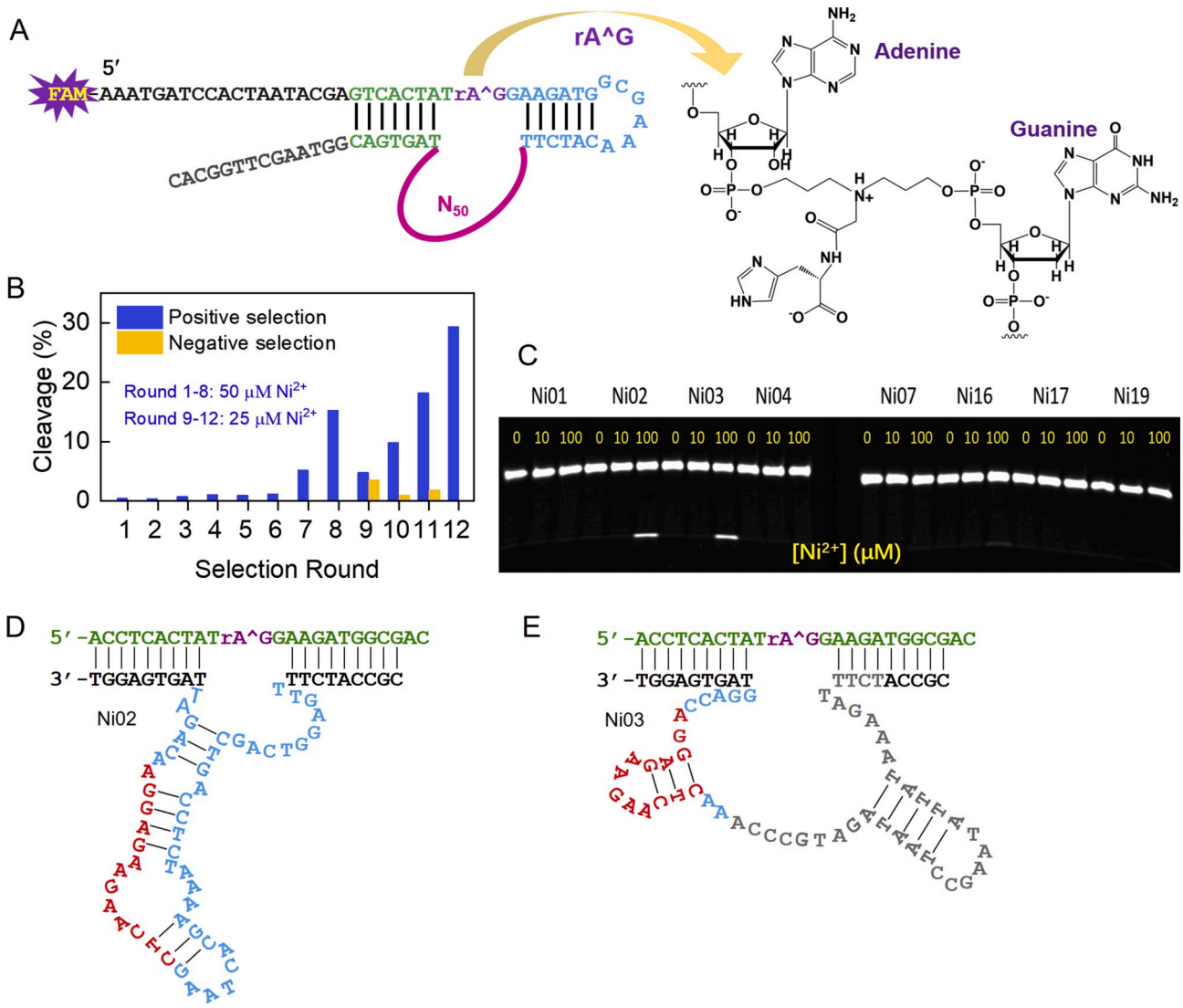


**Fig. 1.** (A) The library sequence before the cleavage step and the structure of the modified rA^G cleavage junction. (B) The progress of the selection. At each round, samples were incubated with $Ni^{2+}$ for 1 h in 25 mM NaCl, 50 mM MOPS, pH 7.5 for the positive selections. From round 9 to 11, negative selections were also carried out in the same buffer but without $Ni^{2+}$. (C) A gel-based assay of the eight sequences tested. Each sample was incubated with 0, 10 or 100 μM of $Ni^{2+}$ in 25 mM NaCl 50 mM MOPS, pH 7.5 for 1 h. The lanes with a lower band contained active DNAzymes. The secondary structure of the trans-cleaving (D) Ni02 and (E) Ni03 DNAzymes, and the conserved nucleotides are marked in red. The gray part in (E) was later truncated. (For interpretation of the references to color in this figure legend, the reader is referred to the Web version of this article.)

DNAzymes are DNA-based catalysts and most DNAzymes require metal ions for activity (Hwang et al., 2016; Liu et al., 2017; Ma and Liu, 2020; Silverman, 2016). Efforts have been made to obtain DNAzymes that can work in the presence of specific metal ions for metal sensing. Since 1994, various DNAzymes have been obtained to detect $Pb^{2+}$ (Breaker and Joyce, 1994; Peng et al., 2019; Yang et al., 2020), $Zn^{2+}$ (Gu et al., 2013; Huang et al., 2020; Li et al., 2000; Santoro et al., 2000), $UO_2^{2+}$ (Liu et al., 2007), $Hg^{2+}$ (Hollenstein et al., 2008), $Cd^{2+}$ (Huang and Liu, 2015), $Na^{+}$ (Torabi et al., 2015; Zhou et al. 2015, 2016), trivalent lanthanides (Huang et al., 2016), and other metals (Liu et al., 2003; Torabi et al., 2015; Zhou et al., 2017). DNAzymes exhibit high catalytic activities that allow signal amplification and robust rate-based measurement, enabling high sensitivity (Gong et al., 2015; Lake et al., 2019; Zhang et al., 2011). Enzymatic reactions may also avoid the non-specific metal binding problem of aptamers (He et al., 2018).

Selection of $Ni^{2+}$-specific DNAzymes has not yet been carried out, although $Ni^{2+}$ was mixed with other metal ions to form a soup for selection (Liu et al., 2003). $Ni^{2+}$ can activate the 17E DNAzyme, although the activity is very low compared to other divalent transition metals such as $Zn^{2+}$ and $Co^{2+}$ (Li et al., 2000). Given the low but still measurable activity with 17E, the likelihood of re-selecting the 17E or the related 8–17 DNAzyme is high if we directly use $Ni^{2+}$ on a standard library (Schlosser and Li, 2010). To avoid this problem, a modified library might be used. We recently obtained a series of $Zn^{2+}$-specific DNAzymes by introducing a single glycyl–histidine-functionalized tertiary amine moiety at the cleavage junction (de Rochambeau et al., 2018; Huang et al., 2020). Such a single modification at the fixed region is advantageous for selection and application, since the standard PCR process can be used and the cost of synthesis is relatively low (Huang and Liu, 2015, 2016; McConnell et al., 2020b; Morrison et al., 2018). Since this nitrogen-rich ligand may also have a high affinity for $Ni^{2+}$, we herein performed a new selection using this modified library for $Ni^{2+}$ and developed a biosensor using the resulting DNAzyme.

## 2. Materials and methods

**Chemical.** The DNA sequences for in vitro selection were purchased from Integrated DNA Technologies (Coralville, IA, USA). The

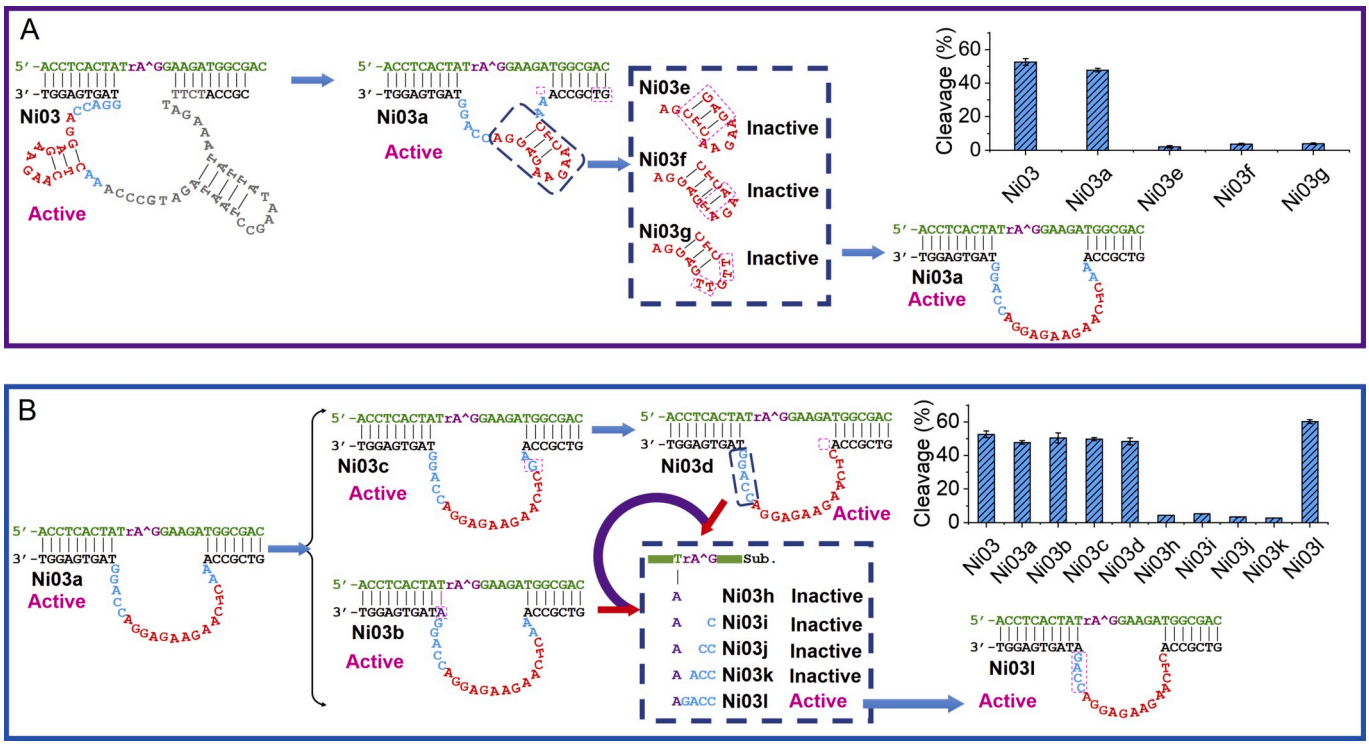


**Fig. 2.** Truncation and mutation of the Ni03 DNAzyme. (A) Truncation of the gray part and the test of the hairpin structure in red. The cleavage activity of each mutant is summarized in the bar plot. (B) Starting from the Ni03a mutant for further truncation of the DNAzyme. The activity of the mutants is summarized in the bar plot. The reactions were performed in 50 mM MOPS, pH 8.0 for 2 h with 100 μM $Ni^{2+}$. The mutated regions based on the previous mutant are shown in the pink boxes. (For interpretation of the references to color in this figure legend, the reader is referred to the Web version of this article.)

oligonucleotides containing the modified cleavage junction were synthesized and characterized as described previously (Huang et al., 2020). The other DNA samples used in this work were from Eurofins (Huntsville, AL, USA). All the metal salts, Tris(hydroxymethyl)aminomethane (Tris), 3-(*N*-morpholino)propanesulfonic acid (MOPS), and 4-(2-hydroxyethyl)-1-piperazineethanesulfonic acid (HEPES) were purchased from Sigma–Aldrich and Mandel Scientific (Guelph, ON, Canada). Milli-Q water was used to prepare all buffers and solutions.

**In vitro section.** The method of in vitro selection has been described by our group with some modification (Huang et al. 2014, 2020). For each selection round, modified DNA library was dissolved in buffer B (25 mM NaCl, 50 mM MOPS, pH 7.5). After incubating with $Ni^{2+}$ (25 μM–50 μM in different rounds, see Table S2) at room temperature, the reaction was quenched with 8 M urea and the cleaved product was purified and extracted. The selected DNA was re-suspended in 60 μL HEPES buffer (5 mM, pH 7.5) before two PCR steps were used to obtain the library for subsequent round of selection. For negative selections, the library was incubated with the same buffer but without $Ni^{2+}$, and the noncleaved sequences were harvested for the next positive selection with $Ni^{2+}$.

**Enzyme assays.** Gel-based assays were performed with the carboxyfluorescein (FAM)-labeled glycyl-histidine modified substrate (5 μM) and an enzyme (7.5 μM) in buffer B. The samples were annealed at 95 °C for 1 min followed by slow cooling to 4 °C for 30 min. The annealed DNAzyme was then diluted 5-fold in buffer (total 5 μL), and then 2 μL $Ni^{2+}$ (or other metals) was added to initiate the cleavage reaction. At designated time points, the reaction was quenched by adding the gel loading buffer (7 μL, 5 mM EDTA, 8 M urea). The products were then separated by 15% denaturing polyacrylamide gel electrophoresis (dPAGE) at 200 V for 80 min and analyzed using a Bio-Rad ChemiDoc MP imaging system. All assays were run at least in duplicate and the data obtained were fitted according to the first-order rate equation $Y_t = Y_0 + a(1\text{-}e^{-kx})$, where $Y_t$ and $Y_0$ are the cleavage fraction at a given reaction time $t$ and 0 min, respectively; $a$ is the fitting coefficients; and $k$ is the observed rate constant. When the cleavage fraction was less than 20% after 13 h, the rate constant was estimated as $k$ = cleavage fraction/$t$.

**Sensing.** The stock sensor was prepared by annealing the FAM-labeled substrate (5 μM) and the quencher-labeled enzyme (15 μM) in 50 mM HEPES with 100 mM NaCl, pH 7.5 at 95 °C for 1 min followed by slow cooling to 4 °C. The sample was then stored in a −20 °C freezer overnight. The annealed DNAzyme (1 μL, 5 μM) in 50 mM MOPS at pH 8.0 (4 μL) was mixed with a final concentration of 10–100 μM $Ni^{2+}$ or other metal ions (2 μL) to initiate the cleavage reaction for 2 h. The products were diluted to 100 μL with 100 mM NaCl, 1.5 mM HEPES, pH 7.5. This solution was then diluted to 200 μL with Milli-Q water. The samples were excited at 485 nm, and fluorescence emission from 500 nm to 650 nm was collected using a FluoroMax-4 spectrofluorometer (Horiba Jobin Yvon). The sensor response in Lake Ontario water was prepared by mixing the Lake Ontario water with buffer at 1:1 ratio, and the other operations were the same.

## 3. Results and discussion

**In Vitro Selection of a $Ni^{2+}$-specific DNAzyme.** To isolate a $Ni^{2+}$-specific DNAzyme, in vitro selection was carried out with a library containing 50 random nucleotides as described previously (Huang et al., 2020), and the main difference was that $Ni^{2+}$ was used as the metal ion (Fig. S1). The structure of the cleavage junction with a nitrogen-rich glycyl-histidine modified ligand is shown in Fig. 1A, and we named the new junction (rA^G) (de Rochambeau et al., 2018), where rA denotes for ribo-adenine. This modified linkage contained an imidazole and a carboxyl group, which may provide multiple metal binding sites. Since RNA is more susceptible to cleavage (Li and Breaker, 1999), cleavage most likely takes place at this position. After adding $Ni^{2+}$, a fraction of the library might be cleaved resulting in a shorter sequence, which was readily harvested by a denaturing gel electrophoresis and

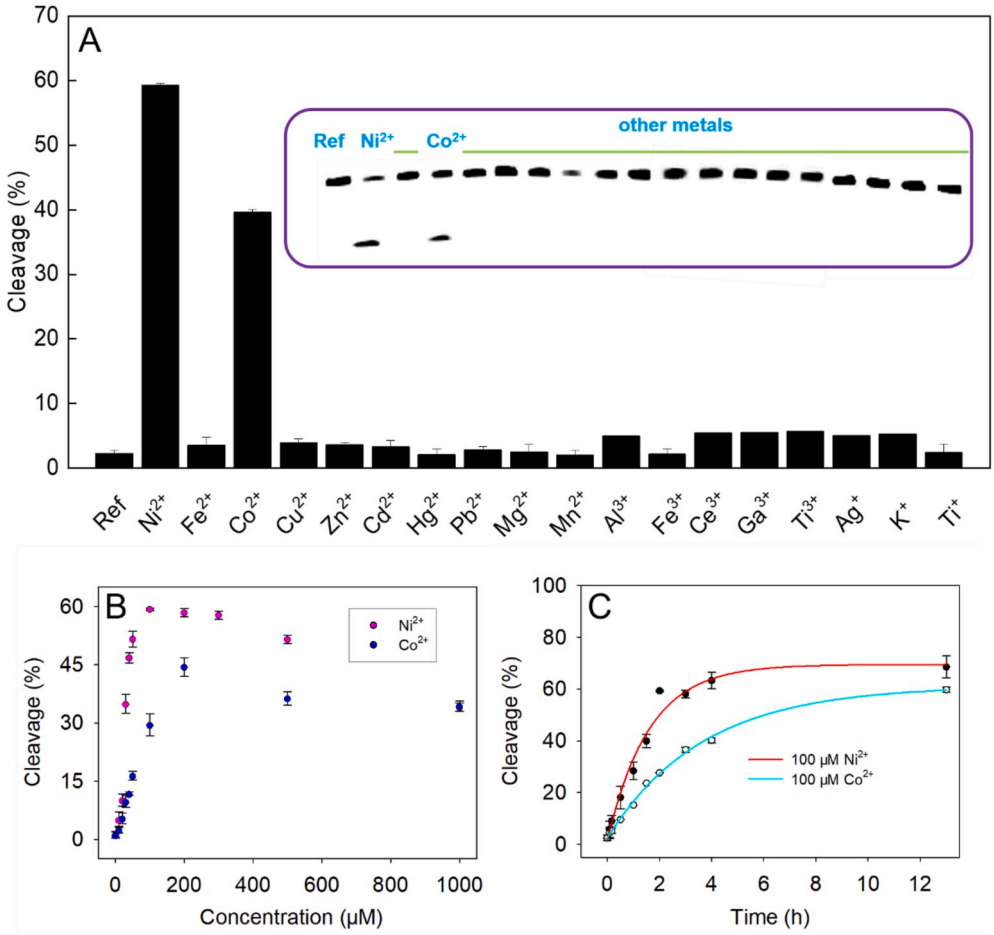


**Fig. 3.** (A) Ni03l reacting with 100 μM different metals after 2 h. Inset: the corresponding gel micrograph. (B) Fraction of cleavage as a function of $Ni^{2+}$ or $Co^{2+}$ concentration after a 2 h reaction. (C) Kinetics of Ni03l in the presence of 100 μM $Ni^{2+}$ or $Co^{2+}$. All of the reactions were performed in 50 mM MOPS, pH 8.0.

amplified using two rounds of PCR to reconstruct the library for the next round of selection. To avoid nonspecific cleavage, we carried out negative selections from round 9 to 11 (Fig. 1B), where just the selection buffer was used (no $Ni^{2+}$ added), and the remaining uncleaved population were harvested for the next positive $Ni^{2+}$ selection. The cleavage yield increased gradually and reached 29.3% at round twelve (Fig. 1B and Table S2), when we stopped the reaction and sequenced the library.

We obtained a total of 28,302 well-aligned sequences. The most abundant 18 families accounted for 42.7% of them (Fig. S2). We predicted the secondary structure of each family (Zuker, 2003), and tested eight of them for activity in the trans-cleaving form using a FAM-labeled substrate (Fig. 1C). Ni02 and Ni03 showed about 20% cleavage with 100 μM $Ni^{2+}$ after 1 h. The analyzed sequences contained a conserved motif of CTCAAGAAGAGGA. Since this sequence was predicted by Mfold to be in a stable stem region in Ni02 (Fig. 1D), we focused our attention on Ni03 (Fig. 1E). The Ni03 sequence represented 5.42% of the final sequenced library (Fig. S2).

**Truncation and optimization.** Since Ni03 has a large catalytic loop, we first tried to truncate it to make it a smaller DNAzyme (Fig. 2A and Fig. S3). The Ni03a was obtained by deleting the entire gray region of Ni03, which greatly shortened Ni03 while still maintained a high activity with $Ni^{2+}$ (see the bar plot in Fig. 2A).

Since a hairpin structure was predicted in the conserved region in Ni03a, we then wanted to test this structure using three mutants: Ni03e swapping the three base pairs, Ni03f extending the paired region, and Ni03g mutating the four A bases to four T bases in the loop. The purpose of these three mutants was to test if the hairpin structure was important or not. However, none of the mutants were active, arguing against a hairpin structure. Therefore, we believe that the structure of Ni03a should be a large loop without the predicted base pairs as shown in the bottom right corner of Fig. 2A.

Based on Ni03a, we aimed to further optimize and truncate it (Fig. 2B). First, an adenine base was inserted to extend the stem by pairing it with the T in the substrate strand (Ni03b), which still maintained a high cleavage activity. At the same time, we tested the Ni03c by mutating the adenine in the right end of the enzyme loop to a guanine, which was still active. Therefore, we suspected these two adenines in blue were unimportant and we deleted them and produced Ni03d, which was indeed still active. Based on Ni03b and Ni03d, we wanted to further truncate the structure by gradually deleting the longer loop in blue (Ni03h, Ni03i, Ni03j, Ni03k, and Ni03l). Among them, only Ni03l maintained a high cleavage activity (about 60%, see the bar plot in Fig. 2B). The final optimized Ni03l structure is shown in the bottom right part of Fig. 2B. The catalytic loop has only 17 nucleotides and is rich in purine. For the NiCo riboswitches, the metal binding site is created in part by the positioning of nucleophilic groups from conserved guanine nucleotides (Furukawa et al., 2015). Small asymmetric purine-rich loops that contain a G-A interaction may represent a divalent metal ion binding site in RNA (Hofmann et al., 1997; Wrzesinski and Ciesiolka, 2005). In our DNAzyme, similar interactions might also take place considering this purine rich sequence.

**Characterization of the Ni03l DNAzyme.** Since the Ni03l appeared to be a minimal DNAzyme, we then further characterized it. For $Ni^{2+}$ sensing, metal specificity is important. We tested Ni03l in the presence of 100 μM of different metal ions (Fig. 3A). Ni03l is quite specific for $Ni^{2+}$ (~60% cleavage), and it had almost no cleavage with other metals

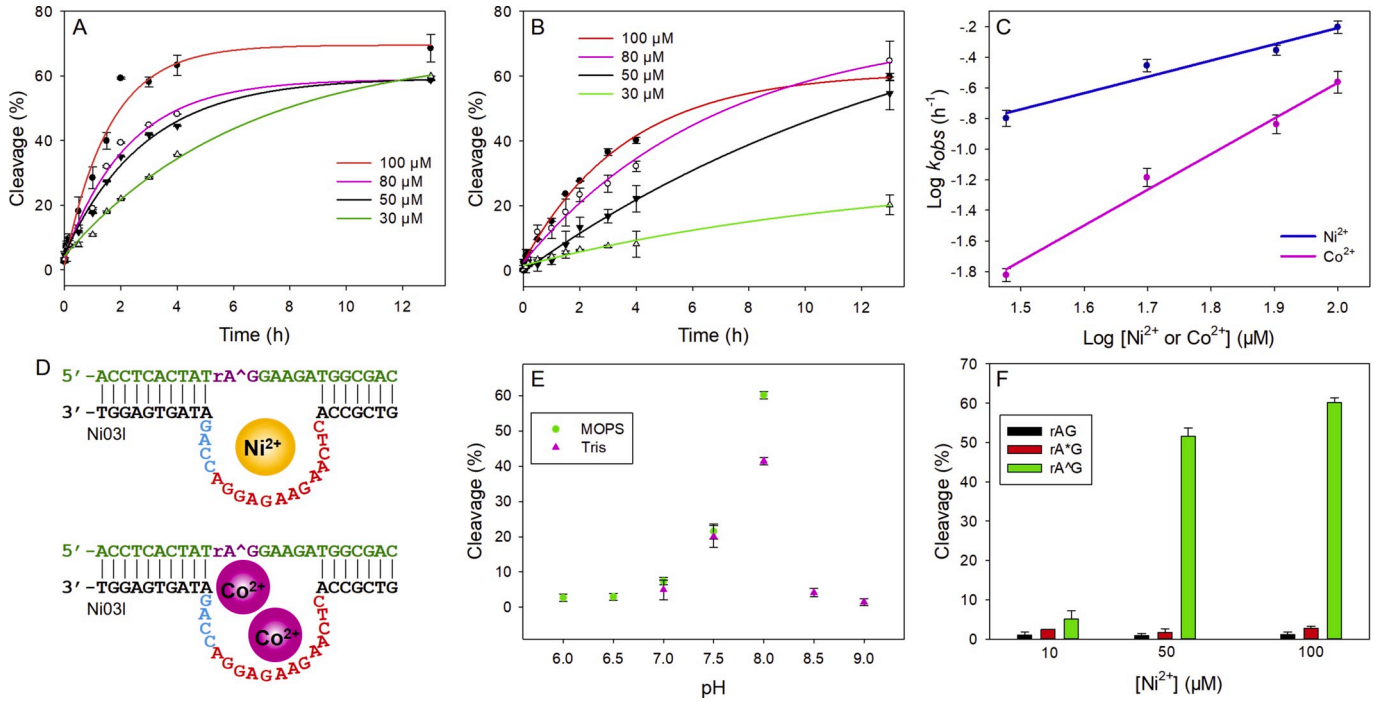


**Fig. 4.** Kinetics of cleavage by Ni03l with different concentrations of (A) $Ni^{2+}$ and (B) $Co^{2+}$. (C) Double log plots of rate constant versus [$Ni^{2+}$] or [$Co^{2+}$] for Ni03l. (D) Schemes showing the DNAzyme using one $Ni^{2+}$ or two $Co^{2+}$ ions for catalysis. (E) Cleavage yield of Ni03l with 100 μM $Ni^{2+}$ in different pH after 2 h reaction. (F) Cleavage yield of Ni03l DNAzyme for the three types of substrates in the presence of 10, 50, and 100 μM $Ni^{2+}$ after a 2 h reaction. All of the reactions were performed in 50 mM MOPS, pH 8.0 except for the pH effect.

except for $Co^{2+}$ (~40%). We then tested various concentrations of $Ni^{2+}$and $Co^{2+}$ by measuring the cleavage yield at 2 h. At each concentration, $Ni^{2+}$ showed higher cleavage yield than $Co^{2+}$ (Fig. 3B). The most optimal concentration was 100 μM $Ni^{2+}$ (cleavage yield ~60%). At even higher $Ni^{2+}$ concentrations, inhibition was observed, which might be attributable to nonspecific $Ni^{2+}$ binding to DNA bases, inducing denaturation or misfolding of the DNAzyme. We also measured the cleavage kinetics (Fig. 3C), and the first-order cleavage rate constants were 0.63 $h^{-1}$ with 100 μM $Ni^{2+}$, and 0.27 $h^{-1}$ with 100 μM $Co^{2+}$.

Since this inserted metal ligand might bind multiple metal ions (Huang et al., 2020), we wanted to quantitatively measure the number of $Ni^{2+}$ ions involved in Ni03l. We measured the cleavage rate at different $Ni^{2+}$ and $Co^{2+}$ concentrations. Ni03l had higher rates of cleavage at higher $Ni^{2+}$ or $Co^{2+}$ concentrations (Fig. 4A and B). We fitted each kinetic data and obtained the rate constants ($k$). With 100 μM $Ni^{2+}$, we obtained a rate constant $k$ of 0.63 $h^{-1}$. In Fig. 4C, we made a double log plot of [$Ni^{2+}$] or [$Co^{2+}$] versus log$k$, and its slope is $n$, the number of $Ni^{2+}$ or $Co^{2+}$ required for the reaction. The slope was 1.06 for $Ni^{2+}$, and 2.33 for $Co^{2+}$, suggesting that it used one $Ni^{2+}$ or two $Co^{2+}$ ions for catalysis (Fig. 4D). Therefore, the mechanism of the reaction (e.g. recruiting metal ions for interacting with the scissile phosphate in the transition state for charge neutralization) was different for these two metal ions. For the NiCo riboswitch, binding is not a simple one-to-one interaction between RNA and $Co^{2+}$ or $Ni^{2+}$, but rather involves the cooperative binding of more than one cation by each aptamer (Furukawa et al., 2015).

$Ni^{2+}$ and $Co^{2+}$ are very similar to each other, and this similarity was reflected in many nucleic acid based ligands. For example, for the aptamer in the NiCo riboswitch, the dissociation constants were determined to be of 5.6 μM for $Co^{2+}$ and 12 μM for $Ni^{2+}$ (Furukawa et al., 2015). An in vitro selected $Ni^{2+}$-binding aptamer showed a similarly high affinity ($K_d$ ~ 1 μM) to $Ni^{2+}$ as to $Co^{2+}$ (Hofmann et al., 1997). On the other hand, the $K_d$ for a $Co^{2+}$-binding aptamer (no. 18) investigated by the elution of RNA from metal ion affinity column was about 3.1 mM (Wrzesinski and Ciesiolka, 2005). The formation of a stable RNA aptamer-biocytin complex mediated by $Ni^{2+}$ was moderately inhibited in the presence of $Co^{2+}$ (Seetharaman et al., 2001). The cleavage of hammerhead ribozyme cleaved 12–14% in the presence of 20 μM $Ni^{2+}$ or $Co^{2+}$ (Markley et al., 2001). Our results also showed that even with the modified metal ligand, it is still quite difficult to tell these two metals apart.

We then studied the effect of pH (Fig. 4E). The cleavage yields were measured after 2 h, and higher pH produced higher cleavage yields up to pH 8. When the pH was further increased, the cleavage decreased. Therefore, high pH is more favorable for the reaction, which might be related to the deprotonation of the 2′-OH of the RNA base, making it a better nucleophile (Dahm et al., 1993; Saran and Liu, 2016). In addition, we found that MOPS was more suitable for the cleavage activity based on comparing the cleavage yields at pH 8, likely due to chelation of $Ni^{2+}$ by the primary amine in Tris. At pH 8, the background cleavage in the absence of metal ions was still very low (Fig. S4).

To confirm that the importance of the modified cleavage junction, we also studied the effect of the junction base composition. The current junction is denoted by rA^G as shown in Fig. 1A. When it was replaced by a normal rAG (typical phosphodiester linkage) or rA*G (phosphorothioate modified), the cleavage activities of Ni03l with $Ni^{2+}$ were fully abolished (Fig. 4F). Thus, the inserted metal ligand is critical for the cleavage activity.

**A biosensor for $Ni^{2+}$ detection.** After understanding the structure and activity of the Ni03l DNAzyme, we then tested its performance as a biosensor for $Ni^{2+}$. To design the biosensor, the 3′-end of the substrate strand was labeled with a FAM fluorophore, and the 5′-end of the enzyme was labeled with a dark quencher. This DNAzyme complex had a low fluorescence in this initial state due to the proximity of the two labels. Cleavage was expected to separate the fluorophore from the quencher to enhance fluorescence.

We incubated this sensor with various metal ions to test for selectivity. As shown in Fig. 5A and B, the fluorescence enhancement was observed mainly with $Ni^{2+}$ and $Co^{2+}$ as expected. It is interesting to note that the natural riboswitch can also recognize both $Ni^{2+}$ and $Co^{2+}$

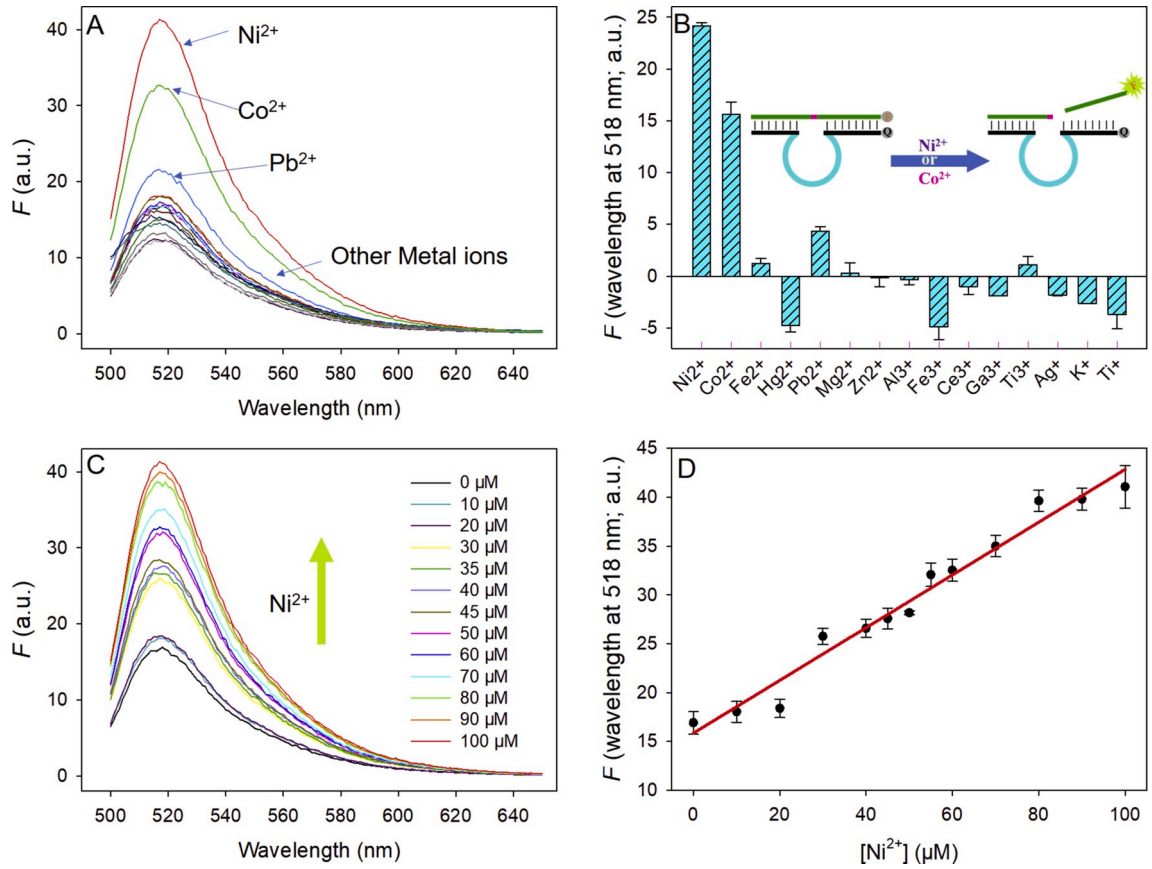


**Fig. 5.** (A) Sensor specificity tests with 100 μM of metal ions after 2 h incubation. (B) Fluorescence enhancement at λ = 518 nm with different metal ions. Insert: Schematic representation of the Ni03l DNAzyme beacon design. (C) Fluorescence spectra of the sensor after incubation with different concentrations of $Ni^{2+}$ for 2 h. (D) Fluorescence enhancement with different $Ni^{2+}$ concentrations (the reaction concentration). The error bars represent the standard deviation from three independent measurements.

(Furukawa et al., 2015). Some metals showed decreased fluorescence attributable to fluorescence quenching by them. We reason that it is possible to use another DNAzyme, such as 17E, to help distinguish $Ni^{2+}$ and $Co^{2+}$. 17E has a higher activity with $Co^{2+}$ (~7-fold higher in cleavage rate constant than $Ni^{2+}$ at 100 μM concentration) (Li et al., 2000). We have also confirmed the much higher activity of 17E in the presence of $Co^{2+}$ in Fig. S5. By using multiple DNAzymes, the specificity can be further improved (Huang and Liu, 2014; Liu and Lu, 2007).

In addition, $Ni^{2+}$ concentration-dependent fluorescence enhancement was observed (Fig. 5C). The change in the fluorescence peak at λ = 518 nm is plotted against $Ni^{2+}$ concentration (Fig. 5D). We obtained a detection limit of 12.9 μM $Ni^{2+}$ based on a calculation of 3σ/slope, which was higher than the toxic level of $Ni^{2+}$ in drinking water (1.7 μM), and thus water samples need to be concentrated to directly use this sensor. More likely, this sensor may find applications for detecting $Ni^{2+}$ in wastewater from mining and plating, which contain higher concentration of $Ni^{2+}$. For example, the samples from 57 treatment plants in Michigan showed that range in Ni was 12–800 mg/kg (about 200 μM–14 mM). Nickel is present in effluents of electroplating industries in the range of 20–200 ppm (about 340 μM–3.4 mM) (Revathi et al., 2005). The nickel wastewater from an electroplating factory in Jordan had a $Ni^{2+}$ concentration of 12.48 mg/L (about 210 μM) (Salem and Awwad, 2014). The acceptable limit of Ni in industrial discharge wastewater is 2 mg/L (34 μM) (Sharma et al., 1991). According to the Ni data from the industries, our designed sensor based on Ni03l with a detection limit of 12.9 μM $Ni^{2+}$ might be useful to detect Ni in these industry fields. To assess the robustness of this sensor, water from Lake Ontario was also tested (Fig. S6). A similar response was observed for the spiked water samples and $Ni^{2+}$ still reached a limit of detection of 15.9 μM.

We have searched the literature for $Ni^{2+}$ sensors (Table S3), and most small organic molecule based sensors were tested in organic solvents or contained a fraction of solvent. Those that measured in water were strongly interfered by many other divalent metal ions. To achieve a high sensitivity, the sensors had to be immobilized on some solid support. Our DNAzyme-based sensor was tested in water without immobilization, and it was only interfered by $Co^{2+}$. While previous efforts have been made to obtain aptamers and riboswitches for $Ni^{2+}$, they have not yet been converted to biosensors for detection. When nucleic acid based sensors are considered, our DNAzyme is the first tested as a biosensor for $Ni^{2+}$.

## 4. Conclusions

In conclusion, we reported the first nickel-specific RNA-cleaving DNAzymes, which were evolved by an in vitro selection effort using $Ni^{2+}$ as the metal cofactor. The success of this selection was attributed to the metal binding ligand introduced at the cleavage site. The Ni03 DNAzyme was studied in detail and was truncated to obtain Ni03l, which still maintained high activity with $Ni^{2+}$. Ni03l shows high selectivity for $Ni^{2+}$ and only $Co^{2+}$ showed activity among the other tested metal ions. Interesting, Ni03l binds one $Ni^{2+}$ ion but two $Co^{2+}$ ions, indicating that it has different mechanisms of using these two metal ions. We have also demonstrated the use of Ni03l for selectively sensing $Ni^{2+}$ with a detection limits of 12.9 μM $Ni^{2+}$. The proposed sensor was also tested in a real water sample, and the results agreed well with the analysis using the buffer. This work indicated the single metal ligand modified strategy can be a general method to obtain sensing DNAzymes, and it also represents the first nucleic acid based biosensor for $Ni^{2+}$.

## Declaration of competing interest

The authors declare that they have no known competing financial interests or personal relationships that could have appeared to influence the work reported in this paper.

## CRediT authorship contribution statement

**Wei Ren:** Investigation, Methodology, Writing - review & editing. **Po-Jung Jimmy Huang:** Investigation, Methodology, Writing - review & editing. **Donatien de Rochambeau:** Writing - review & editing. **Woohyun J. Moon:** Investigation. **Jinyi Zhang:** Investigation. **Mingsheng Lyu:** Supervision. **Shujun Wang:** Supervision. **Hanadi Sleiman:** Conceptualization, Writing - review & editing. **Juewen Liu:** Conceptualization, Writing - review & editing.

## Acknowledgment

We thank funding from the National Key Research and Development Program of China (2018YFC0311106), the Best in Science program of the Ministry of Environment and Climate Change of Ontario, the Global Water Futures project of the Canada First Research Excellence Fund (CFREF), and Natural Sciences and Engineering Research Council of Canada (NSERC). Wei Ren was supported by the Priority Academic Program Development of Jiangsu Higher Education Institutions (PAPD) to visit the University of Waterloo.

## Appendix A. Supplementary data

Supplementary data to this article can be found online at https://doi.org/10.1016/j.bios.2020.112285.

## References

Alizadeh, K., Rezaei, B., Khazaeli, E., 2014. Sensor. Actuator. B Chem. 193, 267–272.
Breaker, R.R., Joyce, G.F., 1994. Chem. Biol. 1, 223–229.
Dahm, S.C., Derrick, W.B., Uhlenbeck, O.C., 1993. Biochemistry 32, 13040–13045.
de Rochambeau, D., Sun, Y., Barlog, M., Bazzi, H.S., Sleiman, H.F., 2018. J. Org. Chem. 83, 9774–9786.
Denkhaus, E., Salnikow, K., 2002. Crit. Rev. Oncol. Hematol. 42, 35–56.
Dubal, D.P., Gomez-Romero, P., Sankapal, B.R., Holze, R., 2015. Nano Energy 11, 377–399.
Furukawa, K., Ramesh, A., Zhou, Z., Weinberg, Z., Vallery, T., Winkler, W.C., Breaker, R. R., 2015. Mol. Cell. 57, 1088–1098.
Gong, L., Zhao, Z., Lv, Y.-F., Huan, S.-Y., Fu, T., Zhang, X.-B., Shen, G.-L., Yu, R.-Q., 2015. Chem. Commun. 51, 979–995.
Gu, H., Furukawa, K., Weinberg, Z., Berenson, D.F., Breaker, R.R., 2013. J. Am. Chem. Soc. 135, 9121–9129.
He, Y., Chen, D., Huang, P.-J.J., Zhou, Y., Ma, L., Xu, K., Yang, R., Liu, J., 2018. Nucleic Acids Res. 46, 10262–10271.
Hofmann, H.-P., Limmer, S., Hornung, V., Sprinzl, M., 1997. RNA 3, pp. 1289–1300.
Hollenstein, M., Hipolito, C., Lam, C., Dietrich, D., Perrin, D.M., 2008. Angew. Chem. Int. Ed. 47, 4346–4350.
Huang, P.-J.J., de Rochambeau, D., Sleiman, H.F., Liu, J., 2020. Angew. Chem. Int. Ed. 59, 3573–3577.
Huang, P.-J.J., Liu, J., 2014. Anal. Chem. 86, 5999–6005.
Huang, P.-J.J., Liu, J., 2015. Nucleic Acids Res. 43, 6125–6133.
Huang, P.-J.J., Liu, J., 2016. Anal. Chem. 88, 3341–3347.
Huang, P.-J.J., Vazin, M., Lin, J.J., Pautler, R., Liu, J., 2016. ACS Sens. 1, 732–738.
Huang, P.-J.J., Vazin, M., Liu, J., 2014. Anal. Chem. 86, 9993–9999.
Hwang, K., Hosseinzadeh, P., Lu, Y., 2016. Inorg. Chim. Acta. 452, 12–24.
Kahn, J.S., Hu, Y., Willner, I., 2017. Acc. Chem. Res. 50, 680–690.
Lake, R.J., Yang, Z.L., Zhang, J.L., Lu, Y., 2019. Acc. Chem. Res. 52, 3275–3286.
Li, H., Cui, Z., Han, C., 2009. Sensor. Actuator. B Chem. 143, 87–92.
Li, J., Zheng, W., Kwon, A.H., Lu, Y., 2000. Nucleic Acids Res. 28, 481–488.
Li, Y., Breaker, R.R., 1999. J. Am. Chem. Soc. 121, 5364–5372.
Liu, J., Brown, A.K., Meng, X., Cropek, D.M., Istok, J.D., Watson, D.B., Lu, Y., 2007. Proc. Natl. Acad. Sci. U.S.A. 104, 2056–2061.
Liu, J., Lu, Y., 2007. J. Am. Chem. Soc. 129, 9838–9839.
Liu, M., Chang, D., Li, Y., 2017. Acc. Chem. Res. 50, 2273–2283.
Liu, Z., Mei, S.H., Brennan, J.D., Li, Y., 2003. J. Am. Chem. Soc. 125, 7539–7545.
Ma, L., Liu, J., 2020. iScience 23, 100815.
Markley, J.C., Godde, F., Sigurdsson, S.T., 2001. Biochemistry 40, 13849–13856.
McConnell, E.M., Cozma, I., Morrison, D., Li, Y., 2020a. Anal. Chem. 92, 327–344.
McConnell, E.M., Morrison, D., Rincon, M.A.R., Salena, B.J., Li, Y.F., 2020b. TrAC Trends Anal. Chem. 124, 115785.
Morrison, D., Rothenbroker, M., Li, Y.F., 2018. Small Methods 2, 1700319.
Peng, D., Li, Y., Huang, Z., Liang, R.-P., Qiu, J.-D., Liu, J., 2019. Anal. Chem. 91, 11403–11408.
Qing, Z., Xu, J., Hu, J., Zheng, J., He, L., Zou, Z., Yang, S., Tan, W., Yang, R., 2019. Angew. Chem. Int. Ed. 58, 11574–11585.
Revathi, M., Kavitha, B., Vasudevan, T., 2005. J. Environ. Sci. Eng. 47, 1–6.
Salem, N.M., Awwad, A.M., 2014. J. Saudi Chem. Soc. 18, 379–386.
Santoro, S.W., Joyce, G.F., Sakthivel, K., Gramatikova, S., Barbas, C.F., 2000. J. Am. Chem. Soc. 122, 2433–2439.
Saran, R., Liu, J., 2016. Anal. Chem. 88, 4014–4020.
Schlosser, K., Li, Y., 2010. Chembiochem 11, 866–879.
Seetharaman, S., Zivarts, M., Sudarsan, N., Breaker, R.R., 2001. Nat. Biotechnol. 19, 336–341.
Sharma, Y., Prasad, G., Rupainwar, D., 1991. Int. J. Environ. Sci. 37, 183–191.
Sigel, R.K., Sigel, H., 2010. Acc. Chem. Res. 43, 974–984.
Silverman, S.K., 2016. Trends Biochem. Sci. 41, 595–609.
Tedsana, W., Tuntulani, T., Ngeontae, W., 2015. Anal. Chim. Acta 867, 1–8.
Torabi, S.-F., Wu, P., McGhee, C.E., Chen, L., Hwang, K., Zheng, N., Cheng, J., Lu, Y., 2015. Proc. Natl. Acad. Sci. U.S.A. 112, 5903–5908.
Wrzesinski, J., Ciesiolka, J., 2005. Biochemistry 44, 6257–6268.
Yang, H., Peng, D., Zhou, Y., Liu, J., 2020. Chembiochem. https://doi.org/10.1002/cbic.202000073.
Zhang, J., Lan, T., Lu, Y., 2020. TrAC Trends Anal. Chem. (Reference Ed.) 124.
Zhang, X.-B., Kong, R.-M., Lu, Y., 2011. Annu. Rev. Anal. Chem. 4, 105–128.
Zhou, W., Saran, R., Chen, Q., Ding, J., Liu, J., 2016. Chembiochem 17, 159–163.
Zhou, W., Saran, R., Liu, J., 2017. Chem. Rev. 117, 8272–8325.
Zhou, W., Zhang, Y., Huang, P.-J.J., Ding, J., Liu, J., 2015. Nucleic Acids Res. 44, 354–363.
Zuker, M., 2003. Nucleic Acids Res. 31, 3406–3415.